Pertanika J. Sci. & Technol. 29 (1): 59 - 75 (2021)

PERTANIKA JOURNALS

SCIENCE & TECHNOLOGY

Journal homepage: http://www.pertanika.upm.edu.my/

Harmonic Current Distortion Using the Linear Quadratic Regulator for a Grid-Connected Photovoltaic System

Oscar Andrew Zongo[1]* and Anant Oonsivilai[2]

[1]Walailak University International College, Walailak University, 222 Thaiburi, Tha sala, Nakhon Si Thammarat, Thailand
[2]School of Electrical Engineering, Suranaree University of Technology, 111 University Avenue, Muang, Nakhon Ratchasima, Thailand

ABSTRACT

This paper presents a comparison between a proportional-integral controller, low pass filters, and the linear quadratic regulator in dealing with the task of eliminating harmonic currents in the grid-connected photovoltaic system. A brief review of the existing methods applied to mitigate harmonic currents is presented. The Perturb & Observe technique was employed for maximum power point tracking. The PI control, low pass filters, and the linear quadratic regulator are discussed in detail in terms of their control strategies. The grid current was analyzed in the system with all three of the controllers applied to control the voltage source inverter of the solar photovoltaic system connected to the grid through an L filter and LCL filter and simulated in MATLAB/SIMULINK. The simulation results obtained have proven the robustness of the linear quadratic regulator over other methods. The technique lowers the grid current total harmonic distortion from 7.85% to 2.13%.

Keywords: Harmonic current distortion, linear quadratic regulator, nonlinear load, photovoltaic system

ARTICLE INFO

Article history:
Received: 17 August 2020
Accepted: 13 October 2020
Published: 22 January 2021

DOI: https://doi.org/10.47836/pjst.29.1.03

E-mail addresses:
oscar.zongo1981@gmail.com (Oscar Andrew Zongo)
anant.oo141@gmail.com (Anant Oonsivilai)
*Corresponding author

ISSN: 0128-7680
e-ISSN: 2231-8526

INTRODUCTION

Solar photovoltaic (PV) systems convert solar radiation into electrical power (Arora & Arora, 2018). They can be used to supply power to customers as standalone units or connected to the grid. One of the sources of harmonic currents in a PV system is the presence of nonlinear loads (Khomsi et al., 2018). Harmonic currents affect the control of interfaced inverters. The interfaced inverters used in PV systems behave like current sources when they are connected to the main grid (Singh et al., 2018). The voltage source inverter (VSI) is responsible for controlling the power injected into the grid. Therefore, appropriate control strategies are needed for VSI to eliminate the effects of current harmonics which degrade the quality of the output power.

Azzam-Jai and Ouassaid (2018) had shown the effectiveness of active power filters (APF) in dealing with harmonic currents caused by nonlinear loads and power electronic converters. Although the hybrid compensation (HC) method using passive and active filters developed by Naderipoura et al. (2015) solved the power quality problems, it was expensive.

Mohamed et al. (2017) proposed various methods to compensate for current harmonics in the grid-connected PV systems by applying a three-phase voltage-fed shunt active power filter. The conventional p-q theory for the harmonic current distortion presented by Krama et al. (2016) is capable of reducing the total harmonic distortion (THD) of the source current from 23.15% to 3.03% and compensating for the reactive power of the system. Jannesar et al. (2018) proposed a control strategy based on the optimal passive harmonic filter (PHF) to deal with the problem of lower active power and higher voltage total harmonic distortion THDV which led to an increased percentage of harmonic current in the LV distribution system located in Yazd province, Iran. Kumar (2015) used an LCL third-order filter to reduce the THD in the load current to within 1.74% and that of voltage to 0.05%. Active power filters were employed to damp harmonic currents by Colque et al. (2018). Belaidi et al. (2016) used grid current drawn by the nonlinear load to calculate the compensator reference current applying the controller based on the p-q theory. The application of VSI as an active power filter for harmonic current distortion can be found in the work of Bag et al. (2016).

To overcome power quality problems in the distribution system caused by harmonic distortion, Peterson et al. (2017) applied the phasor aggregation technique in a high voltage network of 132 kV. Jain and Singh (2019) used a decoupled network of harmonics to filter out the harmonics from load current, thereby compensating for the reactive power consumed by nonlinear loads. An extended Kalman filter (EKF) state estimator was used to estimate the fundamental load currents in the control strategy developed by Srinivas et al. (2019). Chtouki et al. (2016) compared three passive filters L, LC, and LCL with an LCL filter with series and parallel resistors in the harmonic distortion of the system. A technique known as frequency-domain block least-mean square (FBLMS) was presented

by Kandpal et al. (2017). This method corrects the power factor, regulates the voltage, and drops the harmonic distortion of grid currents to below 5% when applied to the IEEE-519 standard system. A method based on an n-stage second-order generalized integrator phase-locked loop (SOGI-PL) was presented by Pereira et al. (2019). The technique was fast in the selection of the highest harmonic components. Additionally, in the study, copper and magnetic losses caused by the LCL filter were taken into account.

In this present study, a comparison is made of minimizing the effects of harmonic currents using a proportional-integral (PI) controller, low pass filter (LPF), and the linear quadratic regulator (LQR). The focus of this paper is the reduction of grid current THD.

The contribution of this research is the application of the LCL filter and the linear quadratic regulator in the minimization of THD and the control of VSI.

METHODOLOGY

In this work, PI control, LPF, and the LQR are discussed and used to design control schemes to control the grid current. The PV system used for testing, PI control, and LPF control schemes is shown in Figure 1 and includes the PV source, DC/DC boost converter, DC/AC converter, and L filter.

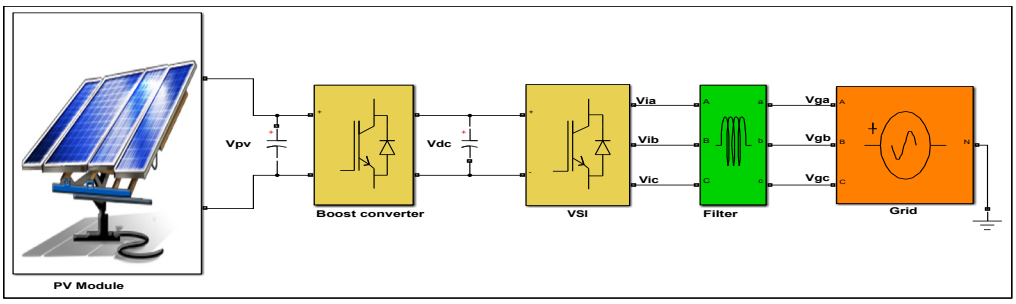

Figure 1. PV system is connected to the grid through VSI

PI Control Scheme

This control methodology is the conventional control strategy that has been used for decades to control several systems. The function of the PI controller (Upaphai et al., 2019) is to make the measured output track the reference input of the controlled system by minimizing the errors between them.

From Figure 1, the grid-side voltage Equation 1 can be written as Fekkak et al. (2018):

$$\begin{bmatrix} v_{ia} \\ v_{ib} \\ v_{ic} \end{bmatrix} = \begin{bmatrix} v_{ga} \\ v_{gb} \\ v_{gc} \end{bmatrix} - L\frac{d}{dt}\begin{bmatrix} i_{ga} \\ i_{gb} \\ i_{gc} \end{bmatrix} \quad (1)$$

Where v_{ia}, v_{ib}, v_{ic} are inverter voltages, v_{ga}, v_{gb}, v_{gc} are grid voltages, i_{ga}, i_{gb}, i_{gc} are grid currents, and L is the filter inductance. The dq transformation of Equations 2 and 3 is,

$$v_{id} = v_{gd} - L\frac{di_{gd}}{dt} + \omega_s L i_{gq} \tag{2}$$

$$v_{iq} = v_{gq} - L\frac{di_{gq}}{dt} + \omega_s L i_{gd} \tag{3}$$

Where:

v_{id} = direct axis inverter voltage.

v_{iq} = quadrature axis inverter voltage.

The abc reference voltages to control the VSI are calculated as shown in Figure 2 (Colque et al., 2018).

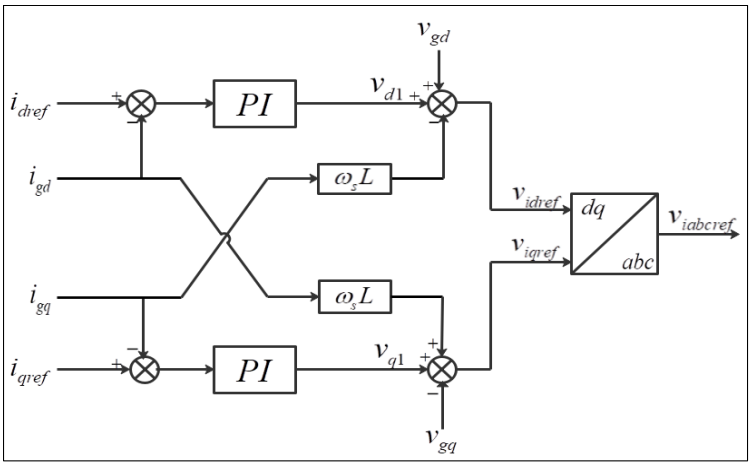

Figure 2. Cross-coupling control of current loops

In Figure 2, the output voltages of the PI-Controllers are (Equations 4 and 5):

$$v_{d1} = k_p\left(1 + \frac{k_i}{s}\right)\left(i_{dreft} - i_d\right) \tag{4}$$

$$v_{q1} = k_p\left(1 + \frac{k_i}{s}\right)\left(i_{qreft} - i_q\right) \tag{5}$$

Therefore, the dq components of the voltage references can be deduced as Equations 6 and 7:

$$v_{dref} = v_{dg} + v_{d1} - \omega_s L i_{iq} \tag{6}$$

$$v_{qref} = v_{qg} + v_{q1} - \omega_s L i_{id} \tag{7}$$

Reference Current Calculation

The active (P) and reactive (Q) powers written in the dq transformation are (Equations 8 and 9):

$$P = \frac{3}{2}\left(v_d i_d + v_q i_q\right) \tag{8}$$

$$Q = \frac{3}{2}\left(v_q i_d + v_d i_q\right) \tag{9}$$

Re-placing i_q and i_q by their references gives Equations 10 and 11,

$$P_{ref} = \frac{3}{2}\left(v_d i_{dref} - v_q i_{qref}\right) \tag{10}$$

$$Q_{ref} = \frac{3}{2}\left(v_q i_{dref} - v_d i_{qref}\right) \tag{11}$$

From Equations 10 and 11, the currents references can be expressed by Equation 12:

$$\begin{bmatrix} i_{dref} \\ i_{qref} \end{bmatrix} = \frac{2}{3\left(v_{id}^2 + v_{iq}^2\right)} \begin{bmatrix} v_{id} & v_{iq} \\ v_{iq} & -v_{id} \end{bmatrix} \begin{bmatrix} P_{ref} \\ Q_{ref} \end{bmatrix} \tag{12}$$

The complete circuit diagram for this method is shown in Figure 3.

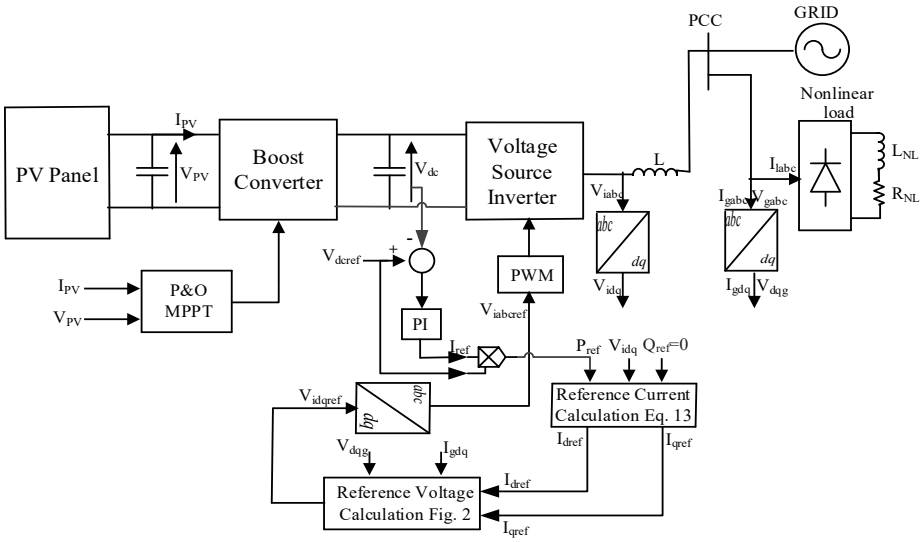

Figure 3. PI control scheme

LPF Control Scheme

In this control mechanism, two LPFs were used to filter the load currents separately and then the filtered currents were subtracted from the original components of the load currents to obtain the harmonic components as shown in Figure 4 (Colque et al., 2018).

Harmonic Current Extraction

The three-phase load currents (i_{la}, i_{lb}, i_{lc}) were converted into their dq components (i_{ld}, i_{lq}) and then the two LPFs were used to filter the currents separately. The filtered currents were subtracted from the original three-phase load currents to obtain the harmonic components as shown in Figure 4 (Colque et al., 2018).

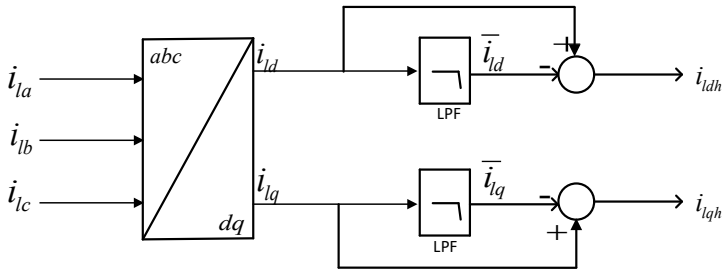

Figure 4. Extraction of harmonic currents

The outputs in Figure 4 are added to the reference currents in Equation 12 to obtain Equations 13 and 14,

$$i_{dreft} = i_{dref} + i_{ldh} \tag{13}$$

$$i_{qreft} = i_{qref} + i_{lqh} \tag{14}$$

These become the new reference currents. The developed control strategy is shown in Figure 5.

LQR Control Scheme

The LCL filter added to the PV system is shown in Figure 6 (Pereira et al., 2019). The filter damps the harmonic currents caused by nonlinear loads and the electronic components in VSI. Proper modeling of the filter is crucial in the design of a suitable controller for the VSI so that it contributes to the mitigation of the THD in the system.

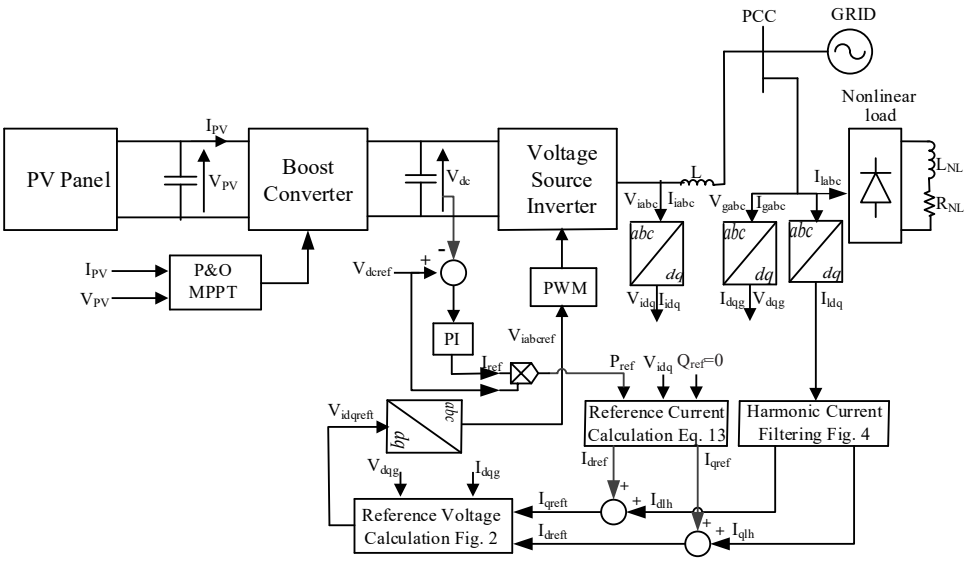

Figure 5. The LPF control scheme

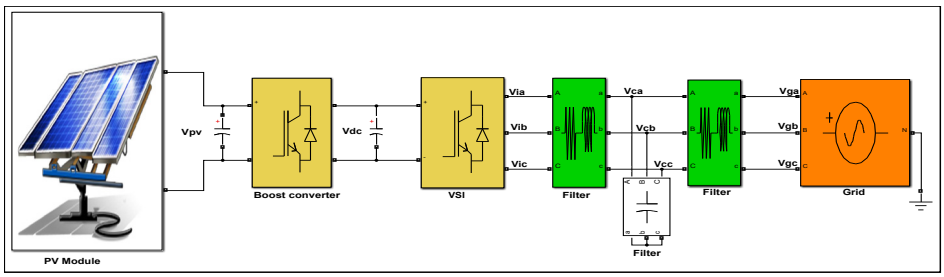

Figure 6. PV system with an LCL filter

Dynamic Model of the VSI and LCL Filter

The equivalent circuit of the LCL filter with damping resistance is shown in Figure 7 (Darwish et al., 2013 & Geddada et al., 2015), in which V_i denotes the inverter voltage; V_C denotes the grid voltage; V_C is the capacitor voltage; R_i, R_g, L_i, and L_g are the filter resistances and inductances, respectively; R_C is the filter capacitance; and R_C is the capacitor damping resistance. The current is flowing from the VSI to the grid.

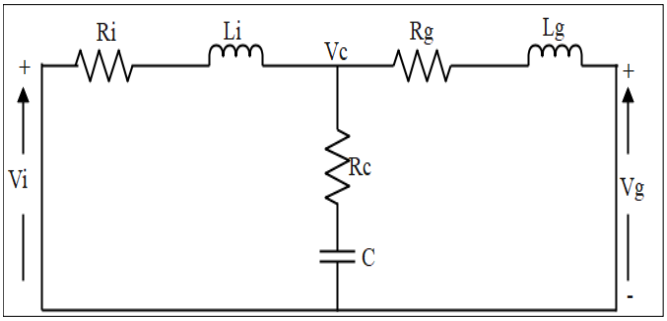

Figure 7. LCL filter equivalent circuit

The per-phase circuit dynamics of Figure 7 can be represented in the stationary reference frame by Equations 15-18

$$L_i \frac{di_i}{dt} = v_i - v_c - R_i i_i \tag{15}$$

$$L_g \frac{di_g}{dt} = v_c - v_g - R_g i_g \tag{16}$$

$$v_c = \frac{1}{C} = \int i_c \cdot dt + i_c R_C \tag{17}$$

$$i_i = i_c + i_g \tag{18}$$

Taking the Laplace transform of Equations 15-18 results in Equation 19,

$$\begin{aligned} i_g(s) = & \frac{sR_C C + 1}{a_0 s^3 + a_1 s^2 + a_2 s + a_3} v_i(s) \\ & - \frac{Cs^2 + CR_i s + 1}{a_0 s^3 + a_1 s^2 + a_2 s + a_2} v_g(s) \end{aligned} \tag{19}$$

The LCL filter transfer function is then defined by Equation 20:

$$G(s) = \frac{i_g(s)}{v_i(s)} = \frac{sR_C C + 1}{a_0 s^3 + a_1 s^2 + a_2 s + a_3} \tag{20}$$

Where:

$$a_0 = L_i L_g C$$
$$a_1 = C\left(L_g\left(R_C + R_i\right) + L_i\left(R_C + R_g\right)\right)$$
$$a_2 = L_g + L_i + C\left(R_C R_i + R_C R_g + R_i R_g\right)$$
$$a_3 = R_i + R_g$$

Where:

i_g = grid-side current,

The LQR can be represented by the block diagram shown in Figure 8. In this controller, r is the reference input, e is the state error, K is the controller gain vector, u is the plant input, P is the controlled plant, x is the state vector, and y is the measured output. In this study, the reference input is the reference grid current i_{gref} ; the state error e is the difference between the reference and the measured grid current i_g ; the controller K is the LQR; and the plant input u is the inverter voltag $V_{i.}$

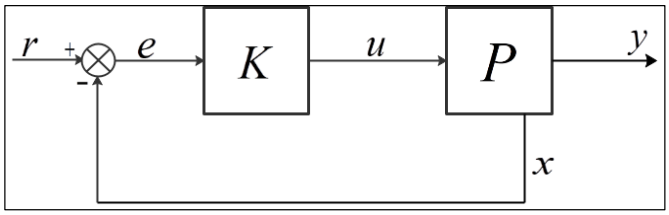

Figure 8. LQR control system

The problem is to find the vector $K(t)$ of the control law (Equation 21) (Xie et al., 2020, Arab et al., 2020 & Oonsivilai et al., 2019),

$$u(t) = -K(t)x(t) \tag{21}$$

that minimizes the value of a quadratic performance index J of the form (Equation 22),

$$J = \int_{t=0}^{t=f} (x'Qx + u'Ru)dt \tag{22}$$

The controller is obtained by solving the Algebraic Riccati Equation (ARE) (Equation 23),

$$\dot{p}(t) = -p(t)A - A'p(t) - Q + p(t)BR^{-1}B'p(t) \tag{23}$$

The closed-loop dynamics under state feedback law with $u(t) = -K(t)x(t)$ is given by Equation 24,

$$\dot{x}(t) = (A - BK)x = A_{CL}x \tag{24}$$

RESULTS, VERIFICATION, AND DISCUSSION

The simulation was performed in MATLAB/Simulink for a grid-connected PV system with the parameters shown in Table 1.

Table 1
Parameters of the PV system

Parameter	Value
The line to line voltage V_{L-L}	380 V
DC bus voltage V_{dc}	650 V
Grid frequency f	50 Hz
Inverter-side resistance R_i	0.5 Ω
Inverter-side inductance L_i	1.7 mH
Grid-side resistance R_g	0.5 Ω
Grid-side inductance L_g	0.1 mH
Filter capacitance R_C	5 μF
Capacitor resistance C	20 Ω

The LCL filter transfer function in Equation 20 was converted into state space. MATLAB function lqr was used to search for the controller K gains used to control the plant. The gains were $K = \begin{bmatrix} 41.4389 & 133.2036 & 255.0779 \end{bmatrix}$.

The step response and linear analysis results of the system with and without LQR are shown in Figure 9 and Table 2 respectively. The step response shows that the system with LQR control is faster, settles to steady-state earlier, and permits lower steady-state error than when the system is without it. The results in Table 2 show that the system with LQR is four times faster than without it, and the difference in steady-state error with and without LQR is significantly big enough to prove the effectiveness of the proposed controller.

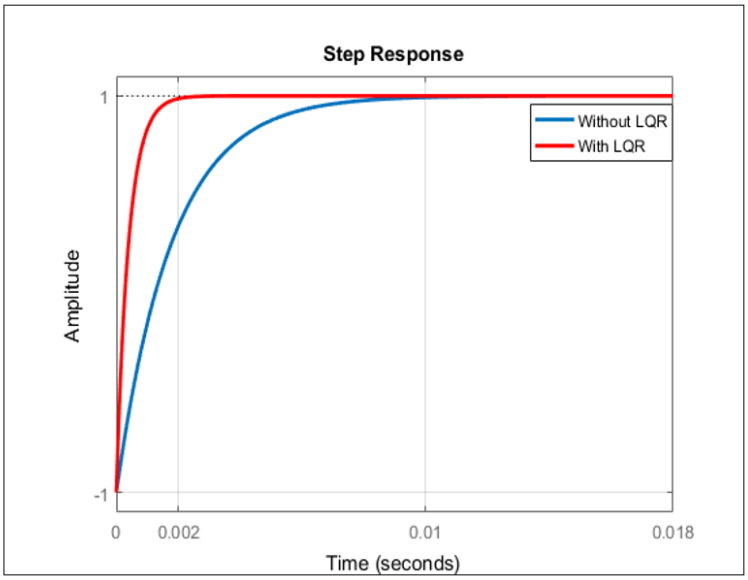

Figure 9. Step response of the system with and without LQR

Table 2

Linear analysis results

Performance	Without LQR	With LQR
Rise time	0.00395	0.000886
Settling time	0.00704	0.00159
Steady state error	1	0.212

RESULTS

The systems which are shown in Figure 3, Figure 5, and Figure 8 were run. The THD recorded with PI control was 7.85% in Figure 10. After the addition of the LPFs in the control strategy, the THD was reduced to 4.27% as shown in Figure 11. Optimal control based on LQR managed to decrease the THD to 2.13% (Figure 12). The results above were verified by the behavior of the grid current shown in Figures 13 to 15.

DISCUSSION

The results presented in Figures 10 to 15 show the robustness of the LQR control strategy compared to the other controllers. With the PI controller, the grid current has serious damaging oscillations.

The application of a filter has shown positive effects in previous studies (i.e., Mohamed et al., 2017; Belaidi et al., 2016; Ouchen et al., 2016) as it also did in this present research

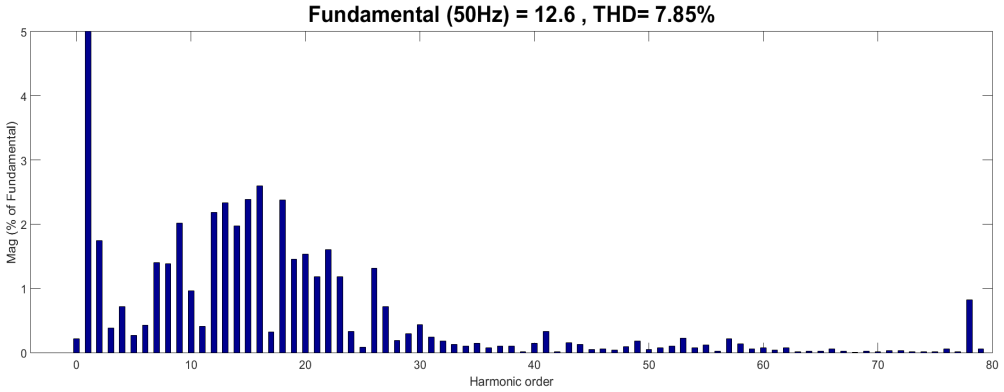

Figure 10. FFT analysis for THD of grid current with the PI control scheme

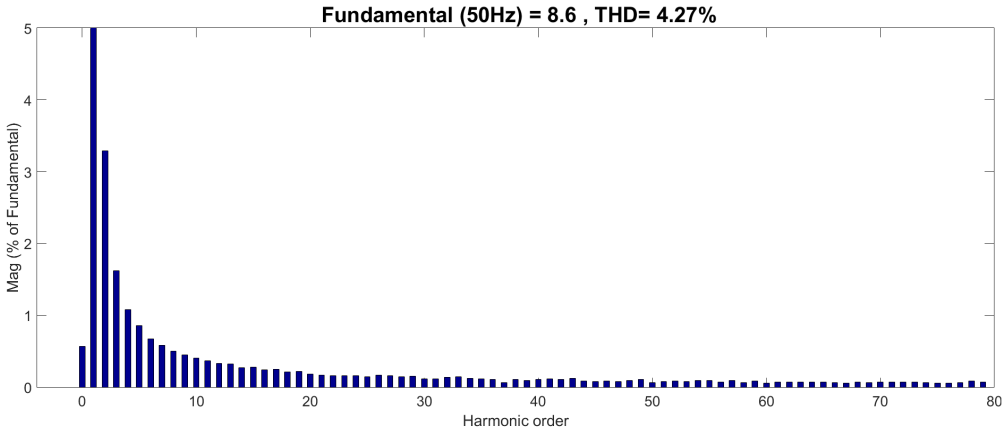

Figure 11. FFT analysis for THD of grid current with the LPF control scheme

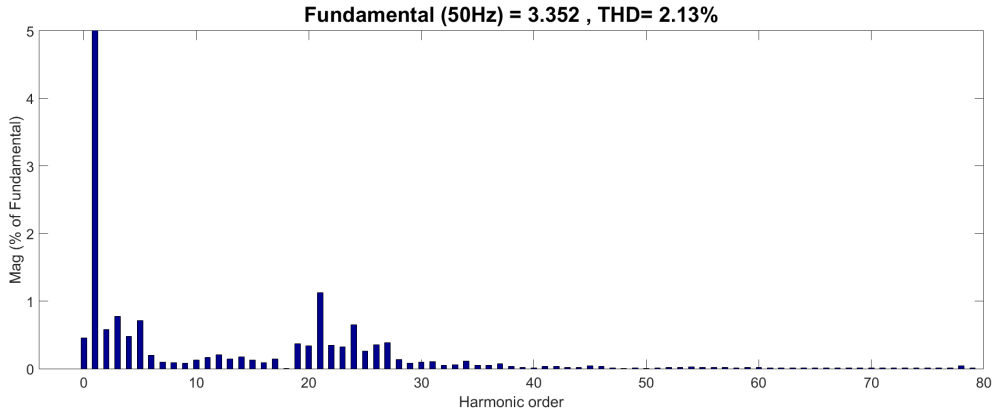

Figure 12. FFT analysis for THD of grid current with the LQR control scheme

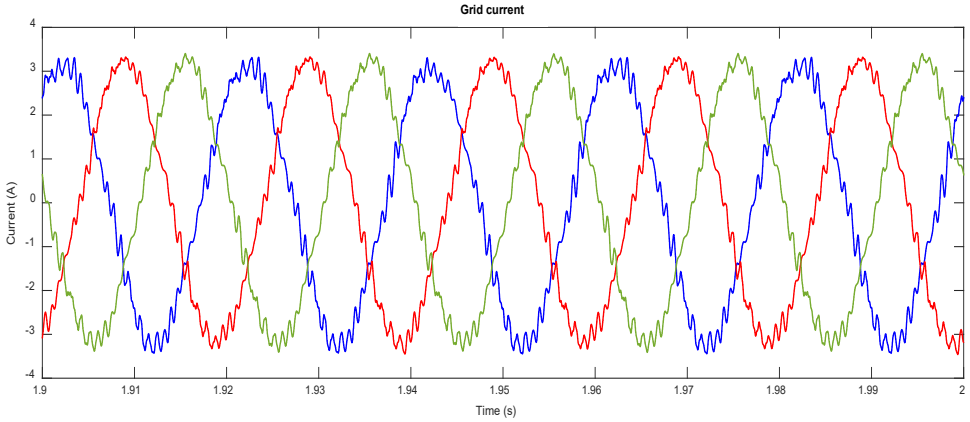

Figure 13. Highly-distorted grid current with a PI controller

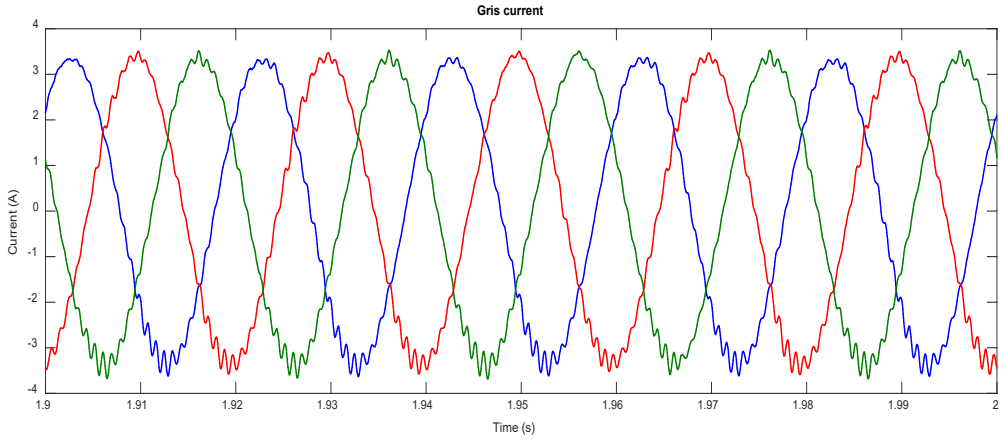

Figure 14. Grid current with the LPF control scheme

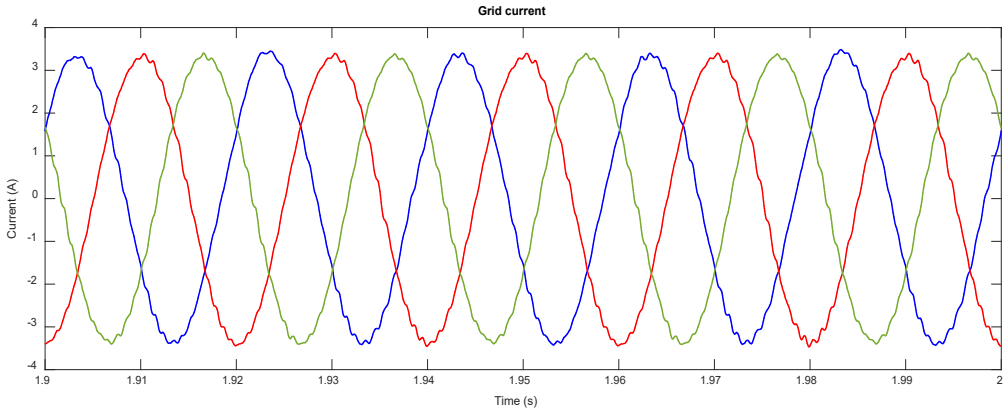

Figure 15. Grid current with the LQR control scheme

even though the control strategies are different. In this research, an LCL filter was used while in the studies of Mohamed et al. (2017), Belaidi et al. (2016) and Ouchen et al. (2016), shunt active power filters were applied. In all cases, THD was highly reduced and there was a significant improvement in the current after the application of the proposed controllers. When LPF and LCL filters were applied, there was a reduction in THD similar to the results obtained by Yousef et al. (2018), in which a shunt active power filter (APF) was applied to eliminate the harmonic currents caused by the nonlinear load. Additionally, there was a significant reduction in harmonic content in the grid current after the application of the LPF scheme (4.27%) and the LQR control (2.13%), meeting the 5% requirement as per the IEEE-519 standard. This experiment had applied LPF and LCL filters with LQR as in the previous study of Pereira et al. (2019), who also employed LCL filters for THD. In both studies, there have been significant distortion of the harmonic currents by the LCL filter. This study had applied L, LPF, and LCL filters in its control schemes, while the study of Chtouki et al. (2016) employed L, LC, and LCL for two comparative studies with and without passive damping. In both types of research, there have been optimum results in terms of harmonic reduction. The use of the L-C-L third-order filter reduced the THD to 1.74%, slightly lower than the results obtained in this work which managed to reduce THD to 2.13% by applying an LCL filter and LQR control for the VSI.

CONCLUSION

The paper has presented a control strategy for VSI that takes care of the presence of harmonics caused by nonlinear loads in the photovoltaic system integrated with the power system. In this paper, the DC/DC converter was controlled by P & O MPPT that concentrated on maximizing the available solar power and maintained an acceptable efficiency around the full load condition. The results obtained from tests with PI, LPF, and an LCL filter with LQR proved the robustness of the proposed controller. The LCL filter and the control scheme based on LQR assisted in removing harmonics from the grid current due to the non-linear load and the VSI. Through the simulation exercise, the total harmonic distortion found in the grid current fell from 7.85% to 2.13% when the optimal controller was applied.

ACKNOWLEDGMENTS

This work is sponsored by Walailak University International College, Walailak University, Nakhon si Thammarat, Thailand.

REFERENCES

Arab, N., Vahedi, H., & Al-Haddad, K. (2020). LQR control of single-phase grid-tied PUC5 inverter with LCL filter. *IEEE Transactions on Industrial Electronics, 67*(1), 297-307. doi: 10.1109/TIE.2019.2897544

Arora, R., & Arora, R. (2018). Experimental investigations and exergetic assessment of 1 kW solar PV plant. *Pertanika Journal of Science and Technology, 26*(4), 1881-1897.

Azzam-Jai, A., & Ouassaid, M. (2018, November 21-23). A multifunctional PV-based shunt active power filter using neural network controller. In *Proceedings of International Symposium on Advanced Electrical and Communication Technologies (ISAECT)* (pp. 1-6). Rabat, Morocco. doi: 10.1109/ISAECT.2018.8618848

Bag, A., Subudhi, B., & Ray, P. K. (2016, January 28-30). Grid integration of PV system with active power filtering. In *Proceedings of 2016 2nd International Conference on Control, Instrumentation, Energy & Communication (CIEC)* (pp. 372-376). Kolkata, India. doi: 10.1109/CIEC.2016.7513810

Belaidi, R., Haddouche, A., Fathi, M., Larafi, M. M., & Kaci, G. M. (2016, November 14-17). Performance of grid-connected PV system based on SAPF for power quality improvement. In *Proceedings of 2016 International Renewable and Sustainable Energy Conference (IRSEC)* (pp. 542-545). Marrakech, Morocco. doi: 10.1109/IRSEC.2016.7984050

Chtouki, I., Zazi, M., Feddi, M., & Rayyam, M. (2016, November 14-17). LCL filter with passive damping for PV system connected to the network. In *Proceedings of 2016 International Renewable and Sustainable Energy Conference (IRSEC)* (pp. 692-697). Marrakech, Morocco. doi: 10.1109/IRSEC.2016.7984020

Colque, J. C., Ruppert, E., & Azcue, J. L. (2018, November 12-14). Performance analysis of a three-phase photovoltaic generation system with active filtering functions connected to the electrical grid. In *Proceedings of 13th IEEE International Conference on Industry Applications (INDUSCON)* (pp. 249-255). São Paulo, Brazil, Brazil. doi: 10.1109/INDUSCON.2018.8627249

Darwish, A., Abdel-Khalik, A. S., Elserougi, A., Ahmed, S., & Massoud, A. (2013). Fault current contribution scenarios for grid-connected voltage source inverter-based distributed generation with an LCL filter. *Electric Power Systems Research, 104*(November 2013), 93-103. doi: https://doi.org/10.1016/j.epsr.2013.06.020

Fekkak, B., Menaa, M., & Boussahoua, B. (2018). Control of transformerless grid-connected PV system using average models of power electronics converters with MATLAB/Simulink. *Solar Energy, 173*(October 2018), 804-813. doi: https://doi.org/10.1016/j.solener.2018.08.012

Geddada, N., Mishra, M. K., & Kumar, M. V. M. (2015). LCL filter with passive damping for DSTATCOM using PI and HC regulators in dq0 current controller for load compensation. *Sustainable Energy, Grids and Networks, 2*(June 2015), 1-14. doi: https://doi.org/10.1016/j.segan.2015.02.001

Jain, V., & Singh, B. (2019). A multiple improved notch filter-based control for a single-stage PV system tied to a weak grid. *Proceedings of 2019 IEEE Transactions on Sustainable Energy, 10*(1), 238-247. doi: 10.1109/TSTE.2018.2831704

Jannesar, M. R., Sedighi, A., Savaghebi, M., Moghaddam, A. A., & Guerrero, J. M. (2018, September 17-21). Optimal passive filter planning in distribution networks with nonlinear loads and photovoltaic systems. In *Proceedings of 20th European Conference on Power Electronics and Applications (EPE'18 ECCE Europe)* (pp. 1-9). Riga, Latvia.

Kandpal, B., Tomar, K. P., Hussain, I., & Singh. B. (2017, October 26-28). Adaptive control of a grid-connected SPV system with DSTATCOM capabilities. In *Proceedings of 4th IEEE Uttar Pradesh Section International Conference on Electrical, Computer, and Electronics (UPCON)* (pp. 452 - 456). Mathura, India. doi: 10.1109/UPCON.2017.8251090

Khomsi, C., Bouzid, M., Jelassi, K., & Champenois, G. (2018, March 20-22). Harmonic current compensation in a single-phase grid-connected photovoltaic system sypplying nonlinear load. In *Proceedings of The 9th International Renewable Energy Congress (IREC)*. Hammamet, Tunisie. doi: 10.1109/IREC.2018.8362520

Krama, A. Zellouma, L., & Rabhi, B. (2016, November 15-17). Improved control of shunt active power filter connected to a photovoltaic system using the technique of direct power control. In *Proceedings of 8th International Conference on Modelling, Identification, and Control (ICMIC)* (pp. 880-885). Algiers, Algeria. doi: 10.1109/ICMIC.2016.7804239

Kumar, D. (2015, March 5-7). Modeling, simulation, and performance analysis of a grid-tied voltage source inverter based photovoltaic system underbalanced and non-linear load conditions. In *Proceedings of 2015 IEEE International Conference on Electrical, Computer, and Communication Technologies (ICECCT)* (pp. 1-5). Coimbatore, India. doi: 10.1109/ICECCT.2015.7225965

Mohamed, J. M., Rasul, A., Khang, H. V., & Kolhe, M. (2017, August 11-14). Harmonic mitigation of a grid-connected photovoltaic system using shunt active filter. In *Proceedings of 20th International Conference on Electrical Machines and Systems (ICEMS)* (pp. 1-5). Sydney, NSW, Australia. doi: 10.1109/ICEMS.2017.8056401

Naderipoura, A., Zinb, A. A. M., Habibuddinc, M. H., Khokhar, S., & Kazemi, A. (2015, October 19-20). Improved control of shunt active power filter using harmony search algorithm. In *Proceedings of 2015 IEEE Conference on Energy Conversion (CENCON)* (pp. 90-95). Johor Bahru, Malaysia. doi: 10.1109/CENCON.2015.7409519

Oonsivilai, A., Zongo, O. A., & Oonsivilai, R. (2019). Stability enhancement of doubly fed induction generator using a linear quadratic regulator. *GMSARN International Journal, 13*(4), 194-201.

Ouchen, S., Abdeddaim, S., Betka, A., & Menadi, A. (2016). Experimental validation of sliding mode-predictive direct power control of a grid-connected photovoltaic system, feeding a nonlinear load. *Solar Energy, 137*(November 2016), 328-336. doi: https://doi.org/10.1016/j.solener.2016.08.031

Pereira, H. A., da Mataa, G. L. E., Xavierc, L. S., & Cupertinob, A. F. (2019). Flexible harmonic current compensation strategy applied in single and three-phase photovoltaic inverters. *Electrical Power and Energy Systems, 104*(January 2019), 358-369. doi: https://doi.org/10.1016/j.ijepes.2018.07.017

Peterson, B., Rens, J., Meyer, J., & Botha, G. (2017, September 20-22). Evaluation of harmonic distortion from multiple renewable sources at a distribution substation. In *Proceedings of 2017 IEEE International Workshop on Applied Measurements for Power Systems (AMPS)* (pp. 1-6). Liverpool, UK. doi: 10.1109/AMPS.2017.8078327

Singh, A. K., Hussain, I., & Singh, B. (2018, January 31-February 2). An improved adaptive P&O technique for two-stage grid interfaced SPVECS. In *Proceedings of 2018 IEEE International Conference on Industrial Electronics for Sustainable Energy Systems (IESES)* (pp. 320-325). Hamilton, New Zealand. doi: 10.1109/IESES.2018.8349896

Srinivas, V. L., Singh, B., & Mishra, S. (2019). Fault ride-through strategy for two-stage GPV system enabling load compensation capabilities using EKF algorithm. *Proceedings of 2019 IEEE Transactions on Industrial Electronics, 66*(11), 8913-8924. doi: 10.1109/TIE.2019.2899546

Upaphai, W., Bunyawanichakul, P., & Janthong, M. (2019). Design of self-tuning fuzzy PID controllers for position tracking control of autonomous agricultural tractor. *Pertanika Journal of Science and Technology, 27*(1), 263-280.

Xie, B., Mao, M., Zhou, L., Wan, Y., & Hao, G. (2020). Systematic design of linear quadratic regulator for digitally controlled grid-connected inverters. *IET Power Electron, 13*(3), 557-567.

Yousef, M. Y., Ismail, M. M., & El-Masry, S. M. (2018, December 18-20). The effect of grid-connected photovoltaic location and penetration level on total harmonic distortion. In *Proceedings of Twentieth International Middle East Power Systems Conference (MEPCON)* (pp. 141-145). Cairo, Egypt. doi: 10.1109/MEPCON.2018.8635252